

SiO₂@LaOF:Eu³⁺ in white light emitting diodes optic efficiency enhancement

Phuc Dang Huu¹, Guo-Feng Luo², Minh Pham Quang³

¹Faculty of Fundamental Science, Industrial University of Ho Chi Minh City, Ho Chi Minh City, Vietnam

²Faculty of Mechanical Engineering, Industrial University of Ho Chi Minh City, Ho Chi Minh City, Vietnam

³Faculty of Mechanical - Electrical and Computer Engineering, School of Engineering and Technology, Van Lang University, Ho Chi Minh City, Vietnam

Article Info

Article history:

Received Jun 18, 2021

Revised Apr 27, 2022

Accepted Jun 1, 2022

Keywords:

Color uniformity

Luminous flux

Mie-scattering theory

SiO₂@LaOF:Eu³⁺

ABSTRACT

The earliest intense red hue compound of SiO₂@LaOF:Eu³⁺ core-shell nanostructures (NS) was created utilizing a basic solvothermal technique and heat processing. The produced core-shell particles are spherical, non-agglomerated, and have restricted size dispersion. Photoluminescence (PL) radiation spectra exhibit sharp maximums in 593, 611, and 650 nm, corresponding with 5D₀ → 7F_J (J=0, 1, 2) Eu³⁺ conversions. The Judd-Ofelt (J-O) hypothesis helps determine the spectrum strength indices and Eu-O ligand activities. The CIE coordinates are x=0.63, y=0.36, nearly equal the NTSC coordinates which are x=0.67, y=0.33. Because of the CCT level of 3475 K, which is lower than 5000 K, this phosphor is appropriate for warm light-emitting diodes. To visualize latent fingerprints both porous and non-porous substrates, the fluorescent labeling marker adapted core-cover SiO₂ (coat III)@LaOF:Eu³⁺ (5 mol%) was utilized. With no background influence, the fingerprints obtained are exceedingly sensible and exclusive, permitting for fingerprint ridge features ranging from level-I to level-III. The findings indicate the significant enhancement in the illumination of corecover NS as a responsive operational nanoparticle for increased forensics and firm status illuminating implementations.

This is an open access article under the [CC BY-SA](https://creativecommons.org/licenses/by-sa/4.0/) license.



Corresponding Author:

Minh Pham Quang

Faculty of Mechanical - Electrical and Computer Engineering, School of Engineering and Technology

Van Lang University

Ho Chi Minh City, Vietnam

Email: minh.pq@vlu.edu.vn

1. INTRODUCTION

Because of their ability to fine-tune features, core-shell configurations have sparked the attention of many scientists and engineers in the latest days. To create varied composite structures, a huge proportion of hard and soft layouts are utilized. Because of its tunable sizes, silica is a common template being used for core-shell structured components [1]-[3]. If nanomaterials are coated as covers of silicate cores, a spherical morphology core-shell phosphor is formed. Furthermore, non-accumulated, ideal hemispheric molded atoms might be primed by fine-adjusting the testing conditions and production techniques, resulting in less scattered light, enhanced brightness, and excellent resolution. These characteristics are helpful for screen technologies, biomedical imagery, and anti-counterfeiting implementations [4]-[6]. Rare earth (RE) treated nano phosphors offer distinct features including crisp absorptivity with radiation streaks in the UV-V is range featuring strong quantum effectiveness, long lifetime and photo - resilience, great heating, and chemical stability, outstanding bio-adaptability, and non-virulence. The following are the quantum performances for lately published oxide hosts: Sr₄Al₁₄O₂₅; Ca₁₄Al₁₀Zn₆O₃₅; CaAl₁₂O₁₉; Sr₄Al₁₄O₂₅:Mn⁴⁺, Na⁺, B³⁺ as

simulated by 450 nm blue-emitted illumination; CdGdAlO₄: Pr³⁺, Yb³⁺. Furthermore, owing to their identical molecular radius, trivalent luminous lanthanide (Ln³⁺) particles may effortlessly integrate to the fluoride-built crystalline structure influenced matrices and exhibit exceptionally optimal brightness at ambient temperature [7]-[9]. Among many RE particles, the Eu³⁺ is the most effective dopant for several hosts in terms of creating red emission, with photo illumination lasting several milliseconds or longer [10]. Rare-earth fluorides have been exceptionally steady substrates for the doping of multiple optically engaged Eu³⁺ particles. These elements have a strong refractive indicator, a weak phonon power, a great ionicity, a high resistance, and an atomic conductivity, leading to the reduced non-radiational degradation and grater illumination quantum performance [11], [12]. Surface modification has been discovered to be among the approaches with the highest proficiency for reducing surface imperfections and non-radiative channels by changing the spacing between radiant and quenching centers. As a result of all of these effects, radiant enhancement is possible in the corecover nano configurations [13]. RE doped nanoparticles having diameters under 100 nm have recently received a lot of attention in surface-based studies, particularly in the acknowledgment of latent fingerprints (LFPs) [14]. It is worth noting that the degrees of image examination are difficult to identify due to these nanomaterials' low fluorescent imaging capacities. As a result, an uncomplicated, low-cost, non-degraded, and accurate method for strain-free observation on non-toxic substances is vital, strongly chemical/thermal durable, high contrasting, great selection, minimal background influence, and enhanced natural LFP fluorescent powders [15].

Because of the restrictions of the latest imagery technicalities and instruments, LFP recognition is based mostly on level II characteristics (including ridgeline completion, bifurcation, and crossing), which is the basis of general recognition. Ensuring the identified precision, level II's amount features set required have to have the range between 6 and 17. Nevertheless, because the dispensation of level II formations over fingertips is unpredictable, precise fingerprint identification requires relatively large fingerprint images. In real circumstances, the obtained LFPs might be unfinished or lack sufficient characteristics. As a result, more fingerprint attributes other than level II are required for greater acknowledgement. Level III qualities (water vapor) on fingertips, in addition to level II formations, are persistent, unchangeable, yet distinct, which might benefit fingermark research [16]. In this study, an optimum core-cover compound of SiO₂@-LaOF:Eu³⁺ phosphorus is utilized as a distinctive luminous marker when observing level I to level III ridgeline layouts over different substrates. The prepared samples were subjected to numerous characterization and optic feature analyses. Anti-counterfeiting and forensic implementations are also thoroughly investigated.

2. METHOD

2.1. Composition of LaOF:Eu³⁺ phosphor

LaOF:Eu³⁺ compounding is formed by chemical reactions between La₂O₃, Eu₂O₃, and LaF₃ [17]. Table 1 calculates the detailed composition of LaOF:Eu³⁺ phosphor. LaOF:Eu³⁺ is made by following these steps: mixing, drying, powderizing, and firing. In order to obtain the best outcome, each step must be taken in the order listed below:

In the beginning, the materials are combined by slurring in the water or methanol. Next, the substance is dried in an air environment and then powdered. The materials were then fired inside capped quartz tubes with N₂ at 1000°C within 1 hour. After that, the product will be powdered again. Now is the time to fire the materials the second time. This step is quite similar to the first one, just only different with the temperature, at 1200°C. After all, we can obtain the ideal LaOF:Eu³⁺.

Table 1. Ingredients of LaOF:Eu³⁺ phosphorus configuration

Materials	By mole %	By grams
La ₂ O ₃	61 (of La)	99.4
Eu ₂ O ₃	5 (of Eu)	8.8
LaF ₃	34	66.6

2.2. Simulation

The implementation of the LightTools 9.0 software and Mie-theory with this research allows WLEDs with dual-film phosphor configurations to be effortlessly modeled by studying phosphor particle scattering, and the method of exploring the effect of SiO₂@LaOF:Eu³⁺ phosphorus on WLEDs effectiveness at the elevated correlating temperatures from 5600 K - 7000 K is assisted, see Figure 1(a) and Figure 1(b). To ensure that the system of WLED in-cup phosphor configuration went perfectly, the SiO₂@LaOF:Eu³⁺ and YAG:Ce³⁺ phosphor composite is shown in the Figure 1(c) and Figure 1(d). As a result, the phosphor film of WLEDs includes SiO₂@LaOF:Eu³⁺ phosphors, YAG:Ce³⁺ phosphorus, and silicon glues.

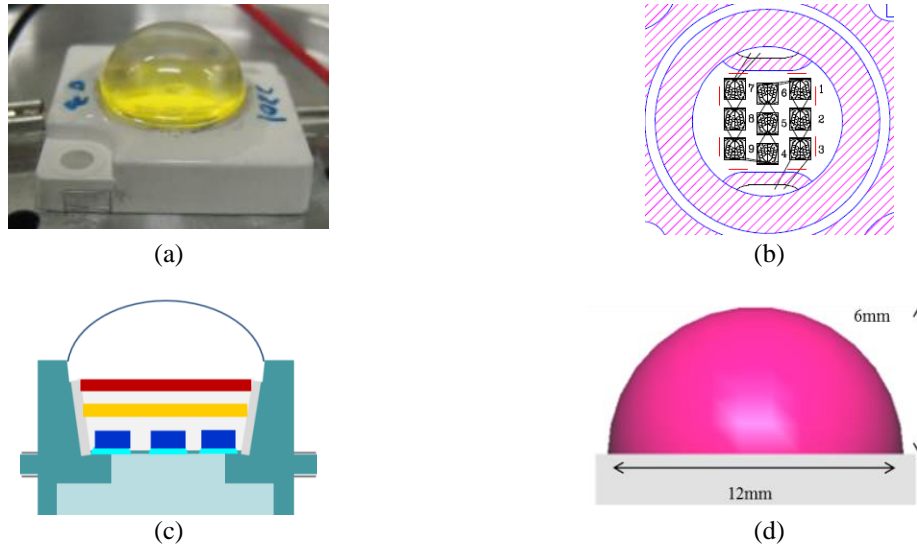


Figure 1. WLEDs configuration demonstration: (a) actual WLEDs, (b) Binding diagram, (c) Pc-WLEDs simulation depiction, and (d) WLEDs modeling using LightTools commercialized program

2.3. Scattering computation

The diffusing factor $\mu_{sca}(\lambda)$, anisotropy element $g(\lambda)$, and decreased diffusing factor $\delta_{sca}(\lambda)$ could be calculated using Mie-scattering theory [18]-[20] using the (1)-(3):

$$\mu_{sca} = \int N(r)C_{sca}(\lambda, r)dr \quad (1)$$

$$g(\lambda) = 2\pi \int_{-1}^1 p(\theta, \lambda, r)f(r)\cos\theta d\cos\theta dr \quad (2)$$

$$\delta_{sca} = \mu_{sca}(1 - g) \quad (3)$$

where $N(r)$ is the diffusive particle dispersing rate (mm^3), C_{sca} denotes the diffusing cross-sections (mm^2), $p(\theta, \lambda, r)$ are respectively the phase-based function, illumination wavelengths (nm), and the diffusing particle radius (m). $f(r)$ is the diffusor size dispersion function in the phosphorous film [21]-[23].

With similar conditions, the core-cover $\text{SiO}_2@\text{LaOF:Eu}^{3+}$ (5 mol %) NS (I - III coatings) PL radiation spectrum as $\lambda_{\text{exc}}=462$ nm would be researched to suit the radiation strengths of the specimen that is not coated. The total emission intensity is found to be increased three times in core-cover NS as much as in un-covered NS. The increased emission strength of core-cover NS is attributed to the shielding impact of the LaOF:Eu^{3+} shell reducing the quantity of non-radiative cores located above the covering of the core SiO_2 . The removal of outlayer -OH groupings because of outer covering has an effect on the radiative relaxation pathway in the core-shell configuration. Even though emission intensity levels may be considerably decreased after III covering, it is well understood that the outer side -OH groups carry an important position in PL quenching. Except for the intensity, the LaOF:Eu^{3+} as well as $\text{SiO}_2@\text{LaOF:Eu}^{3+}$ top location and radiation data are nearly similar. This means the amorphous silica film increases the radiation strengths of $\text{SiO}_2@\text{LaOF:Eu}^{3+}$ owing to illumination absorptivity/diffusing by covered NS, as shown in Figure 2.

Figure 3 depicts the chromaticity coordinates and correlating hue temperatures (CCT) of LaOF:Eu^{3+} (5 mol %) and core-cover $\text{SiO}_2@\text{LaOF:Eu}^{3+}$ (5 mol%) NS (I-III coating) of the Commission Internationale de l'Eclairage (CIE). The coordinates (x, y) of core-cover $\text{SiO}_2@\text{LaOF:Eu}^{3+}$ changed from orange-red-shade (0.521, 0.312) into darker reddish tone (0.521, 0.312). (0.652, 0.338). Furthermore, the un-covered and coated CCT values are computed using the McCamy experimental equation as 1854 and 2332 K, respectively, relatively lower than the data of the basic emission spectra for warm white light.

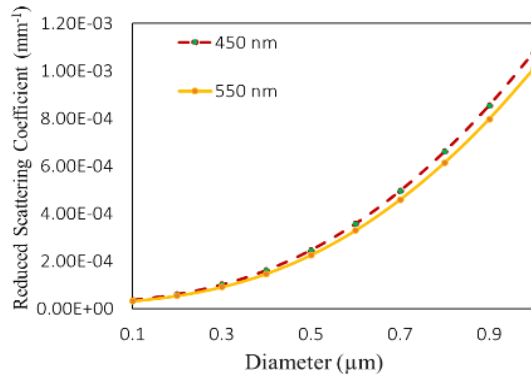


Figure 2. Decreased diffusing factor of SiO₂ ions at 450 nm and 550 nm

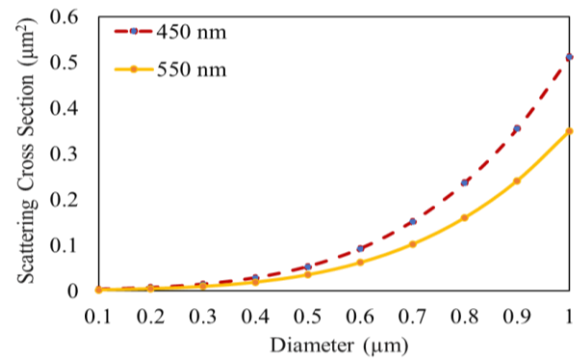


Figure 3. Diffusing cross-section of SiO₂ particles at 450 nm and 550 nm

3. RESULTS AND DISCUSSION

To acquire the complete FPs ridgeline layout identified using the criminal investigation, high-grade phosphorescent dust is necessary. To evaluate its suitability for getting latent FP pictures, the tailored SiO₂@LaOF:Eu³⁺ (5 mol %) (coat III) NS are pigmented onto the LFPs formed beneath standard and 254 nm UV light on numerous un-porous substrates, consisting of the metallic plate, aluminum sheets, blades, and stapler. The illustration indicates that the level II ridge properties (core, bifurcation, hook, eye, dot or island, bridge, fork, ridgeline end-ing) have not been apparent in regular white lighting but are apparent in UV light at 254 nm. With white and 254 nm UV illumination, the improved SiO₂@LaOF:Eu³⁺ is placed to porous flat materials such as cards, magazines in the varied background, and banknotes to examine background intervention. In the FPs viewed beneath UV illumination, the main ridge features are readily obvious. Additionally, the staining of optimal SiO₂@LaOF:Eu³⁺ beneath white-emitting and 254 nm UV illumination is used to study the complete ridge features of single and over-lapped complicated fingerprint pictures. With no background involvement, the various microscopic ridgeline layouts such as center, branching, fusion, hooked, ridge terminating, and enclosing is visible in both lightings. The potential of tailored dust using on the imaging of LFPs on both porous, un-porous materials is illustrated in Figure 4.

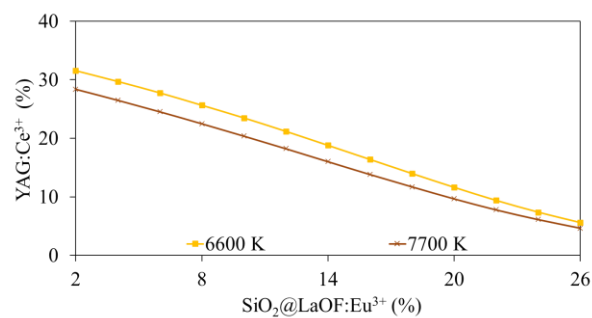


Figure 4. The shift of phosphor concentration for upholding the mean CCTs

To evaluate the fluorescent powders effectiveness, staining the SiO₂@LaOF:Eu³⁺ beneath white-emitting illumination and 254 nm UV light produces a range of overlapping complicated latent fingerprints on aluminum foil surfaces. The figure indicates that underneath regular and 254 nm UV illumination, all three degrees (I-III) of ridge features are apparent, meaning the tailored dust could be successfully a luminous marking reagent for illustrating fingerprints. Furthermore, fingermarks from various contributors are obtained and tainted with enhanced SiO₂@LaOF:Eu³⁺ (coat III) NS utilizing a powder brushing technique beneath white-emitting illumination and also beneath the 254 nm UV irradiation. The three types of fingerprint ridge patterns are central and pocket whorl, as well as ulnar arches. The attain of the high-grade FPs photos post aging days is somewhat beneficial. LFPs stained with SiO₂@LaOF:Eu³⁺ NS on aluminum sheet substrates then aged from one day to one month are shown in Figure 5. FPs tainted with

$\text{SiO}_2@\text{LaOF}:\text{Eu}^{3+}$ NS' standard is substantial in both fresh and aged layouts; great-grade imaging may be owing to latent fingerprint affinity even through aging.

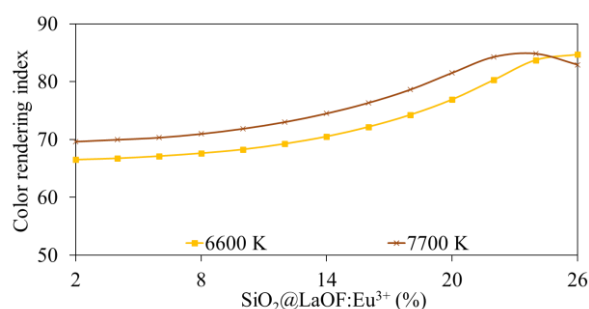


Figure 5. $\text{YAG}:\text{Ce}^{3+}$ concentration functions as WLEDs hue rendering indicator

Considerable efforts have lately been dedicated to the development of anti-counterfeiting technologies. Watermarks, holograms, and barcodes are examples of conventional approaches that have been ineffectual owing to their easy manufacturing techniques and simplicity of duplication. Emerging approaches such as plasmon protection tags, biomimetic microscopic handprints, and magnet-based reactions have the potential to offer greater counterfeit security. To verify authenticity, however, exact and expensive instruments are needed. From the standpoints of security and cost-effectiveness, the luminescence-based method provides increased security and low cost, becoming a popular method among the most well-known methods in terms of anti-duplication areas. Under ultraviolet (UV) illumination, the currency frequently displays luminescence designs. Furthermore, nano ions such as natural chemicals, carbon nanoparticles, and semiconductor substances are used, yet their extended-term toxicity or wide radiation ranges prevent them from being used in other implementations [24]-[26]. But lanthanide-doped nanostructured phosphors exhibit outstanding spectral fingerprints and many benefits, e.g., being hard to make replicas, having minor toxicities, and having great longevity, resulting in their potential implementations in the anticounterfeiting area (see Figure 6). Furthermore, the luminous-based ink is thought to be most suitable for numerous print forms, including dip pen writing, screen scanning, and so on. Figure 7 shows digital pictures of dip pen utilizing tailored core-cover $\text{SiO}_2@\text{LaOF}:\text{Eu}^{3+}$ ink beneath regular, UV 254 nm illumination. UV light reveals sharp and high-intensity pictures that are somewhat hazy with visible illumination. The preceding data support the anti-duplication implementations of core-cover $\text{SiO}_2@\text{LaOF}:\text{Eu}^{3+}$ (5 mol %) NS.

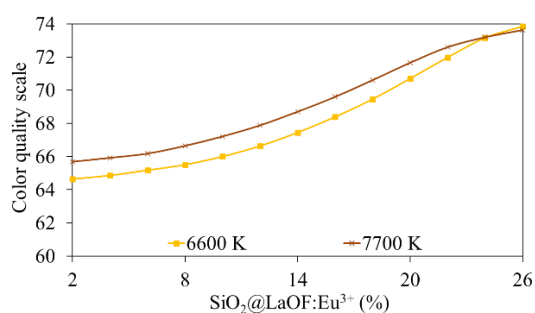


Figure 6. $\text{YAG}:\text{Ce}^{3+}$ concentration functions as WLEDs hue standard ratio

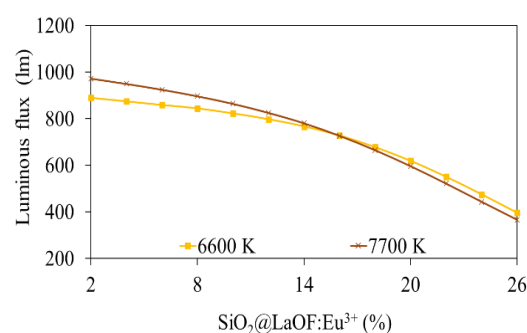


Figure 7. $\text{YAG}:\text{Ce}^{3+}$ concentration functions as WLEDs lighting beam

4. CONCLUSION

A core-cover formed $\text{SiO}_2@\text{LaOF}:\text{Eu}^{3+}$ NS compounding is successfully developed using a simple and low-price modified solvothermal procedure. The $\text{LaOF}:\text{Eu}^{3+}$ PXRD findings showed a pure tetragonal phase with a SiO_2 reaching the peak at 22L. The values of the power range gap and refractive indicator fluctuated non-linear with the concentration of Eu^{3+} . The exterior sheet of oxygen flaws was detected in the

produced composites using EPR. The existence of an 8-nm thick coating core-cover of $\text{SiO}_2@\text{LaOF:Eu}^{3+}$ was revealed by TEM outcomes. The elimination of the surface traps center leads to three times more of the increase in PL intensity in coated NS, leading to a growth in the non-radiative transformation rate. With greater coating cycles, the PL radiation strengths in the core-cover NS could be adjusted. Three coatings of these compounds accomplished a quantum yield reaching up to 56.7%. Because of the increased fluorescence capabilities of the core-cover $\text{SiO}_2@\text{LaOF:Eu}^{3+}$ NS, they might be used as luminescent marking reagents in the LFPs imaging over a diversity of permeable and semi-permeable object interfaces using the dust sweeping technique. These were accomplished by boosting the composite's sticky qualities, keeping it from rapidly oxidizing in air, as well as enhancing the fluorescent features. Regarding greater resolution, fingerprint ridges in detail, simple fluorescence capture, and less background intervention, LFPs visualized using optimal NS outperform commercialized powders. Anti-counterfeiting applications would take advantage of prepared samples as well. Because of these distinct characteristics, prepared core-shell NS may find use in color displays, forensics, and security implementations.

ACKNOWLEDGEMENTS

This study was financially supported by Van Lang University, Vietnam.

REFERENCES




- [1] X. Zheng *et al.*, "Highly solid-luminescent graphitic C3N4 nanotubes for white light-emitting diodes," *J. Phys. D: Appl. Phys.*, vol. 52, no. 50, p. 505503, 2019, doi: 10.1088/1361-6463/ab420b.
- [2] N. Ding *et al.*, "Highly stable and water-soluble monodisperse CsPbX₃/SiO₂ nanocomposites for white-LED and cells imaging," *Nanotechnology*, vol. 29, no. 34, p. 345703, 2018, doi: 10.1088/1361-6528/aac84d.
- [3] L. Peng, Q. Qiping, S. Cao, W. Chen, and T. Han, "Enhancement of luminescence and thermal stability in Sr₂.92-xTmxSiO₅:Eu²⁺ for white LEDs," *Phys. Scr.*, vol. 96, no. 2, p. 025704, 2021, doi: 10.1088/1402-4896/abcf67.
- [4] W. Yindeesuk, S. Sartpan and S. Kamondilok, "The effect of red, blue, green and white light emitting diodes on pigment content and sugar accumulation in wheatgrass," *J. Phys.: Conf. Ser.*, vol. 1719, p. 012085, 2021, doi: 10.1088/1742-6596/1719/1/012085.
- [5] M. A. Alim, M. Z. Abdullah, M. S. A. Aziz, R. Kamarudin, A. P. Irawan, and E. Siahaan "Experimental study on luminous intensity of white LEDs of different configurations," *IOP Conf. Ser.: Mater. Sci. Eng.*, vol. 1007, pp. 012145, 2020, doi: 10.1088/1757-899X/1007/1/012145.
- [6] Q. Xie, Y. Li, X. Min and Y. Ma, "Novel Bromide Quaternary Ammonium Ligand for Synthesizing High Fluorescence Efficiency CsPbBn Perovskite Quantum Dots and Their Fabrication of White Light-Emitting Diodes with Wide Color Gamut," *IOP Conf. Ser.: Mater. Sci. Eng.*, vol. 563, pp. 022047, 2019, doi: 10.1088/1757-899X/563/2/022047.
- [7] N. V. Bharathi, T. Jeyakumaran, S. Ramaswamy and S. S. Jayabalakrishnan, "Synthesis and characterization of self-activated Ba₂V₂O₇ nanophosphor: a potential material for W-LED applications," *Mater. Res. Express*, vol. 6, pp. 106202, 2019, doi: 10.1088/2053-1591/ab3c1d.
- [8] H. Ming, J. Zhang, L. Liu, J. Peng, F. Du and X. Ye, "Luminescent Properties of a Cs₃AlF₆:Mn⁴⁺ Red Phosphor for Warm White Light-Emitting Diodes," *ECS J. Solid State Sci. Technol.*, vol. 7, p. R149, 2018, doi: 10.1149/2.0271809jss.
- [9] T. Jansen, J. Gorobez and T. Jüstel, "Communication—Optical Properties of Red Emitting HK₃SnF₈:Mn⁴⁺ as a Color Converter for Next Generation Warm White LEDs," *ECS J. Solid State Sci. Technol.*, vol. 7, pp. R111, 2018, doi: 10.1149/2.0311806jss.
- [10] Q. Wang *et al.*, "Monolithic semi-polar InGa_n/Ga_n near white light-emitting diodes on micro-stripped Si (100) substrate," *Chinese Phys. B*, vol. 28, no. 8, p. 087802, 2019, doi: 10.1088/1674-1056/28/8/087802.
- [11] K. K. Gupta, S. Som and C. Lu, "Synthesis and luminescence characterization of Ce³⁺ activated Y₂CaAl₂MgZr₂O₁₂ garnet phosphor for white light emitting diodes," *Mater. Res. Express*, vol. 6, pp. 125540, 2019, doi: 10.1088/2053-1591/ab62eb.
- [12] Y. Zhuang *et al.*, "Effect of phosphor sedimentation on photochromic properties of a warm white light-emitting diode," *J. Semicond.*, vol. 39, no. 12, p. 124006, 2018, doi: 10.1088/1674-4926/39/12/124006.
- [13] C. Sun *et al.*, "Highly efficient Mn-doped CsPb(Cl/Br)₃ quantum dots for white light-emitting diodes," *Nanotechnology*, vol. 31, pp. 065603, 2020, doi: 10.1088/1361-6528/ab5074.
- [14] K. Orié and K. Matsushima, "High-quality full-parallax full-color three-dimensional image reconstructed by stacking large-scale computer-generated volume holograms," *Applied Optics*, vol. 58, no. 34, pp. G104-G111, 2019, doi: 10.1364/AO.58.00G104.
- [15] Y. Yuan *et al.*, "High luminous fluorescence generation using Ce:YAG transparent ceramic excited by blue laser diode," *Optical Materials Express*, vol. 8, no. 9, pp. 2760-2767, 2018, doi: 10.1364/OME.8.002760.
- [16] C. Wu *et al.*, "Phosphor-converted laser-diode-based white lighting module with high luminous flux and color rendering index," *Optics Express*, vol. 28, no. 13, pp. 19085-19096, 2020, doi: 10.1364/OE.393310.
- [17] R. G. E. V. I. Batshev, and A. S. Beliaeva, "Design of an optical illumination system for a tunable source with acousto-optical filtering," *Journal of Optical Technology*, vol. 88, no. 2, pp. 66-71, 2021, doi: 10.1364/JOT.88.000066.
- [18] Jin-Wook Shin *et al.*, "Overcoming the efficiency limit of organic light-emitting diodes using ultra-thin and transparent graphene electrodes," *Optics Express*, vol. 26, no. 2, pp. 617-626, 2018, doi: 10.1364/OE.26.000617.
- [19] L. Xiao, C. Zhang, P. Zhong, and G. He, "Spectral optimization of phosphor-coated white LED for road lighting based on the mesopic limited luminous efficacy and IES color fidelity index," *Applied Optics*, vol. 57, no. 4, pp. 931-936, 2018, doi: 10.1364/AO.57.000931.
- [20] T. Wu *et al.*, "Analyses of multi-color plant-growth light sources in achieving maximum photosynthesis efficiencies with enhanced color qualities," *Optics Express*, vol. 26, no. 4, pp. 4135-4147, 2018, doi: 10.1364/OE.26.004135.
- [21] Q. Zhang, R. Zheng, J. Ding, and W. Wei, "Excellent luminous efficiency and high thermal stability of glass-in-LuAG ceramic for laser-diode-pumped green-emitting phosphor," *Optics Letters*, vol. 43, no. 15, pp. 3566-3569, 2018, doi: 10.1364/OL.43.003566.
- [22] O. H. Kwon, J. S. Kim, J. W. Jang, and Y. S. Cho, "Simple prismatic patterning approach for nearly room-temperature processed planar remote phosphor layers for enhanced white luminescence efficiency," *Optical Materials Express*, vol. 8, no. 10, pp. 3230-

3237, 2018, doi: 10.1364/OME.8.003230.




- [23] Y. Tang, Z. Li, G. Liang, Z. Li, J. Li, and B. Yu, "Enhancement of luminous efficacy for LED lamps by introducing polyacrylonitrile electrospinning nanofiber film," *Optics Express*, vol. 26, no. 21, pp. 27716-27725, 2018, doi: 10.1364/OE.26.027716.
- [24] S. Sadeghi, B. G. Kumar, R. Melikov, M. M. Aria, H. B. Jalali, and S. Nizamoglu, "Quantum dot white LEDs with high luminous efficiency," *Optica*, vol. 5, no. 7, pp. 793-802, 2018, doi: 10.1364/OPTICA.5.000793.
- [25] X. Kong, M. Wei, M. J. Murdoch, I. Vogels, and I. Heynderickx, "Assessing the temporal uniformity of CIELAB hue angle," *J. Opt. Soc. Am. A*, vol. 37, pp. 521-528, 2020, doi: 10.1364/JOSAA.384393.
- [26] W. Zhong, J. Liu, D. Hua, S. Guo, K. Yan, and C. Zhang, "White LED light source radar system for multi-wavelength remote sensing measurement of atmospheric aerosols," *Applied Optics*, vol. 58, no. 31, pp. 8542-8548, 2019, doi: 10.1364/AO.58.008542.

BIOGRAPHIES OF AUTHORS






Phuc Dang Huu    received a Physics Ph.D degree from the University of Science, Ho Chi Minh City, in 2018. Currently, he is a lecturer at the Faculty of Fundamental Science, Industrial University of Ho Chi Minh City, Ho Chi Minh City, Vietnam. His research interests include simulation LEDs material, renewable energy. He can be contacted at email: danghuuphuc@iuh.edu.vn.



Guo-Feng Luo    was born in Tainan city, Taiwan. He has been working at the Department of Electrical Engineering, National Kaohsiung University of Science and Technology, Kaohsiung, Taiwan. His research interest is optical material. He can be contacted at email: paradisefall02@gmail.com.



Minh Pham Quang    received the ME degree in Ho Chi Minh City Polytechnic University, he is working as a lecturer at the Faculty of Mechanical - Electrical and Computer Engineering, School of Engineering and Technology, Van Lang University, Ho Chi Minh City, Vietnam. His research interests involve renewable energy, solar energy (grid tie inverter, solar MPPT), power electric, control and automation in factory. He can be contacted at email: minh.pq@vlu.edu.vn.